Targeting CD39 toward activated platelets reduces systemic inflammation and improves survival in sepsis – a preclinical pilot study

Tiago Granja[1], PhD; Andreas Körner[1], MD; Christian Glück[1], MS;
Jan David Hohmann[2], BS; Xiaowei Wang[2,3], PhD; David Köhler[1], PhD;
Ariane Streißenberger[1], BS; Harshal H. Nandurkar[3], MD; Valbona Mirakaj[1], MD;
Peter Rosenberger[1], MD; Karlheinz Peter,[2,3*]MD; Andreas Straub[1*], MD

[1] Department of Anesthesiology and Intensive Care Medicine,
University of Tübingen, Germany
[2]Baker Heart and Diabetes Institute, Melbourne, Australia
[3] Department of Medicine, Monash University, Melbourne, Australia

*both authors contributed equally and share senior authorship

– Supplemental digital content 1 –

Detailed methods description

Blood sampling in human subjects

For *in vitro* experiments, human whole blood was collected by venipuncture with a 21-gauge butterfly needle from an antecubital vein from non-medicated healthy subjects after signed informed consent. The following exclusion criteria for study participation and blood donation

were applied: smokers; drug and medication intake (such as medication which might affect the hemostatic systems and platelets) within 14 days before blood donation; and infectious diseases such as viral hepatitis and human immunodeficiency virus. Blood samples were anticoagulated with citrate in commercially available sampling tubes (S-monovette, Sarstedt, Nümbrecht, Germany). Blood sampling procedures were approved by the ethics committee of the University of Tübingen, Germany.

Effect of different potato apyrase concentrations on platelet–neutrophil aggregate formation and leukocyte activation

Blood samples (90 µl each) were incubated with potato apyrase (PA; Sigma Darmstadt, Germany) in decreasing concentrations (2 U/ml; 0.2 U/ml; 0.02 U/ml; 0.002 U/ml). After five minutes incubation time at 37°C in a waterbath each blood sample was incubated with 5 µl of an ADP solution (Moelab, Langenfeld, Germany) to achieve a final ADP concentration of 20 µM and incubated for further ten minutes at 37°C in the waterbath. Afterwards blood samples were stained with antibodies to determine human platelet–neutrophil aggregate formation and leukocyte CD11b expression in flow cytometry. Expression of the integrin Mac1, as determined by measuring subunit CD11b, on neutrophils is as an indicator for neutrophil activation (1).

Transendothelial migration assay

The effect of apyrase on the ability of neutrophil granulocytes to transmigrate through an endothelial cell layer in the presence of platelets was analyzed according to the principles of a previously described method (2). Briefly, Human dermal microvascular endothelium (HMEC-1) cells were seeded to confluence in a 24-transwell Costar plate with a 3.0 µm flat insert of 6.5 mm diameter (Corning, Krailling, Germany). Neutrophils (1×10^4 cells/well) isolated with Percoll (Sigma) gradient centrifugation were incubated with 2.5×10^7 freshly isolated platelets with 2 U/ml PA and/or 1 µM phorbol 12-myristate 13-acetate (PMA) (Caymanchem,

Michigan, USA) in $HBSS^{+/+}$ (Sigma) as indicated. Platelet–neutrophil aggregates (PNA) were allowed to form and transmigrate for 90 min at 37 ºC with minimal axial agitation. Neutrophils were quantified using a colorimetric method by incubating the azurophilic neutrophil granule protein myeloperoxidase with 2,2-azino-bis (3-ethylbenzothiazoline-6-sulfonic acid) (Sigma).

In vivo sepsis models

Rationale for choosing the respective models

To evaluate drug effects under the *in vivo* conditions of sepsis, we employed a LPS-induced peritonitis model and a cecal ligation and puncture (CLP) model in mice. Both models are described in detail below. The LPS-induced peritonitis sepsis is based on the notion that it is the host's response to bacteria, which leads to mortality and organ failure. The septic response and sepsis-associated multiple organ dysfunction are thought to be secondary to the induction and/or activation of host-derived humoral and cellular immunoinflammatory systems triggered by bacterial products, such as endotoxin. Consequently, endotoxin is considered to be a reasonable surrogate for bacteria (3). Nevertheless, because cytokine responses may differ between an LPS model and bacterial infection we chose to perform further experiments in the CLP model. The CLP model is associated with polymicrobial sepsis and bacteremia. Because of the utility of the CLP model, it has become one of the most common intra-abdominal sepsis models used in studies investigating the pathophysiology and treatment of abdominal sepsis and its systemic consequences (3).

Animals

All *in vivo* experiments were performed with wild-type (WT) C57BL/6NCrl mice (5–10 weeks old, weighing 20–25 g). Mice were obtained from the company Charles River (Sulzfeld/Grabfeld, Germany). All protocols for animal experiments were in accordance with the German guidelines for research on living animals and were approved by the Institutional

Animal Care and Use Committee of the Tübingen University Hospital and the Regierungspräsidium Tübingen, Germany (regional council).

Statement regarding a potential genetic drift in the employed mouse strain

The company Charles River, from which mice were obtained, has established an "International Genetic Standardization" (IGS) Program, to ensure that specific animals have the same genetic profile. Experiments described in this work were performed over approximately two years. Over this time frame the potential occurrence of relevant mutations, which may impact results, can be disregarded.

Pharmacological characteristics of non-targ-CD39 and targ-CD39

Non-targ-CD39 and targ-CD39 have been described previously (4) and were produced in the laboratory of Dr Peter (Baker, Melbourne, Australia). The specificity of targ-CD39 has been evaluated in previous work. To achieve targeting and enrichment of therapeutics on activated platelets, the single-chain antibody (scFv, specific for activated GPIIb/IIIa) SCE5 was used. Originally the scFvSCE5 was selected for its binding to human platelets but also demonstrates a cross-reactivity to mouse platelets. This allows for *in vivo* testing of targ-CD39 in mouse models (4). Due to its blocking effects on GPIIb/IIIa, targ-CD39 may inhibit binding of the JON-A antibody to murine platelets. Targ-CD39 in a concentration of 0.4 µg/g BW, as used in our experiments, provides a strong antithrombotic effect, while leaving the bleeding time unaffected (4), and has also been shown to achieve protection of re-perfused cardiac tissue in an ischemia/reperfusion mouse model (5). The molecular weight of non-targ-CD39 and targ-CD39 lies in the range of 100 kDa (4). Sepsis is characterized by diffuse microvascular leakage, which can affect leakage of plasma constituents and also cellular blood components (6). Under conditions of endothelial barrier destabilization, as it occurs during sepsis (7), it can therefore be expected that non-targ-CD39 and targ-CD39 will extravasate and may

become distributed not only in the blood stream but also in interstitial tissue.

LPS-induced sepsis model

Intravital microscopy of the cremaster microcirculation

Anesthesia was induced in mice by i.p. injection of a mixture of fentanyl (0.05 mg/kg bodyweight (BW)), midazolam (5 mg/kg BW) and medetomidin (0.5 mg/kg BW). Anesthetized mice were placed on a heat pad to maintain their body temperature. The jugular vein was canulated and used to administer experimental agents and additional amounts of the above-described fentanyl–midazolam–medetomidin mixture to maintain anesthesia. Mice were treated by i.p. injection with LPS (Sigma; 0.15 µg/g BW) to induce peritonitis, as well as by i.v. injection of non-targ-CD39 (0.4 µg/g BW), targ-CD39 (0.4 µg/g BW), PA (0,04 U/g BW) or PBS (control) as indicated. A sham group was treated with anesthesia only.

The mouse cremaster preparation was used to study the interaction of leukocytes, platelets, and endothelial cells in the microcirculation according to the principles of a previously described method (8). The cremaster muscle was dissected free of tissue and opened longitudinally with a cautery. Next, the muscle was exposed on a microscope-heated table as a flat trapeze using sutures attached to the tip and edges of the cremaster tissue. The muscle was superperfused with saline throughout the experimental procedure. Postcapillary cremasteric venules with a diameter of 20 to 40 µm and a length of 100 µm were analyzed using an intravital microscope (Nikon Eclipse Ci-L; Nikon, Düsseldorf, Germany) equipped with a black-and-white camera (Hamamatsu Orca R^2, Hamamatsu, Herrsching, Germany) to record multiple films of 30 seconds (sec) length. Platelets and leukocytes were visualized using fluorescent light after i.v. administration of 50 µl rhodamine (0.05%) (Sigma) or 50 µl of the platelet-specific FITC-labeled X488 antibody (emfret, Eibelstadt, Germany).

Four hours after i.p. LPS injection and administration of targ-CD39, non-targ-CD39, PA, or PBS (control), the following parameters were analyzed via intravital microscopy: leukocyte extravasation – defined as the number of leukocytes in the extravascular space surrounding the postcapillary venule; leukocyte rolling velocity – measured within 100 μm vessel length in μm/sec over a time span of 30 seconds; and adherent platelets – defined as green fluorescent objects which connected to the vessel wall over a period of 30 sec.

Analyses of moving and extravasated cells were performed using NIS elements Advanced Research software (Nikon, Düsseldorf, Germany).

Blood and tissue sampling

Blood samples were collected in citrate solution four h after i.p. LPS injection and administration of targ-CD39, non-targ-CD39, PA, or PBS (control) from the right atrium for flow cytometry analysis. Tissue samples from the peritoneum and kidney were collected in 0.4% formalin solution for further histological investigation. All reagents were endotoxin-free.

Tail bleeding times

Tail bleeding times were measured in mice four h after i.p. LPS injection and administration of targ-CD39, non-targ-CD39, PA, or PBS (control) as previously described (4). The tail was transected 5 mm from the tip and immediately submersed in 37 °C saline. The time point when blood flow had ceased for 1 min was measured.

Cecal ligation and puncture

Polymicrobial sepsis was induced in mice using the cecal ligation and puncture procedure (CLP) according to a previously described method (9, 10). Experiments were always

performed in an identical sequence by the same experimenter. Thereby, experimental variability is minimized and CLP-associated bacterial loads can be expected to be nearly identical in all experiments. Mice were anesthetized by i.p. application of ketamin (100 mg/kg BW) and xylazin (5 mg/kg BW). A 1 cm long midline laparotomy was performed to allow exposure of the cecum with adjoining intestine. Approximately one-half of the cecum was tightly ligated with a suture, and the ligated part of the cecum perforated once (through and through) with a 20-gauge needle. The cecum was then returned to the peritoneal cavity and the laparotomy was closed using a suture. Mice were resuscitated with 1 ml of warm physiological saline injected i.p. and returned to their cages with free access to food and water. Targ-CD39, non-targ-CD39, or PA were administered as indicated at the beginning of the experiment and every 48 h thereafter by tail vein injection. Body weights, body temperatures, and mortality of mice were evaluated and recorded in 3-hour intervals throughout the experiment.

PCR

mRNA derived from HMEC-1 cells or murine tissues (peritoneum, kidney, and liver) was isolated with Tri Reagent (Sigma) according to the manufacturer's protocols, and then dissolved and transcribed into cDNA with iScript™ Reverse Transcription Supermix for RT-qPCR (BioRad, Hercules, California, USA). Transcriptional analysis was performed using sybr green (Bio-Rad) in a iCycler CFX96 real-time PCR (BioRad). The annealing temperature of designed primer sets was determined by titration and the calculation of efficiency and slope. Primer sets contained 10 pM of the sense primer and the antisense primer for analysis. Primers were used to amplify in a two-step reaction. Enzyme activation was performed at 95 °C for 3 min, followed by 40 cycles consisting of denaturation at 95 °C for 15 sec, annealing and extension for 45 sec. The ribosome subunit 18S was used for

normalization in studies with HMEC-1 cell lines and murine studies. Primer sequences for analyses of HMEC-1 cells and murine tissue are given in the following list:

Primers for mRNA transcriptional analysis in HMEC cells

Gene name	Accession Nº	Primer	Anneal (ºC)	Melt (ºC)	Size (bp)
IL-6	NM_000600.4	Forward 5'-gacagccactcacctcttca-3' Reverse 5′-caccaggcaagtctcctcat-3'	66.0	80.5	209
18S	NR_003278.3	Forward 5'-gtaacccgttgaaccccatt-3' Reverse 5′-ccatccaatcggtagtagcg-3'	60/62	81.5	151

Primers for mRNA transcriptional analysis in murine tissue

Gene name	Accession Nº	Primer	Anneal (ºC)	Melt (ºC)	Size (bp)
TLR-4	NM_021297.3	Forward 5'-aatccctgcatagaggtagttcc-3' Reverse 5'-atccagccactgaagttctga-3'	62	78	174
TNF-α	NM_013693.3	Forward 5'-tcttctcattcctgcttgtgg-3' Reverse 5′-gatctgagtgtgagggtctgg-3'	62	82.5	142
IL-6	NM_031168.2	Forward 5'-ccggagaggagacttcacag-3' Reverse 5′-ttctgcaagtgcatcatcgt-3'	62	79	166
KC	NM_008176.3	Forward 5'-ctgggattcacctcaagaacatc-3' Reverse 5′-cagggtcaaggcaagcctc-3'	60	82.5	117
CD11b	NM_008401.2	Forward 5'-atggacgctgatggcaatacc -3' Reverse 5′-tccccattcacgtctccca-3'	60	85	203
18S	NR_003278.3	Forward 5'-ccggagaggagacttcacag-3' Reverse 5′-ccatccaatcggtagtagcg-3'	60/62	81.5	151

Flow cytometry

Technical equipment and software

All measurements were performed using a FacsCantoII flow cytometer (Becton Dickinson (BD), Heidelberg, Germany) and FACSDiva software (Version 6, BD). Detailed data analysis

was performed using FlowJo software (version 9.3.2, Ashland-Oregon, USA). All analyses were perfomed in duplicate.

Analysis of human platelet–neutrophil aggregate formation and leukocyte CD11b expression

Human blood samples were collected and prepared for analysis in flow cytometry. An antibody cocktail containing 5 µl anti-CD41 FITC (Beckman Coulter, California, USA), 1 µl anti-CD45 PerCp (Beckman), 1 µl anti-CD66b PE/Cy7 (e-bioscience, Frankfurt-Germany), and 1 µl anti-CD11b BV421 (BD) was prepared and 90 µl of whole blood stained for 30 min at RT, lysed with 1x BD FACS lysing solution (BD), washed with PBS (Sigma), and finally fixed in 50 µl of 1 x BD CellFix® (BD). Flow cytometry analysis was performed within 4 h after staining.

Analysis of murine platelets and leukocytes

The activation and interaction of murine platelets and leukocytes were analyzed according to the principles of a previously described method (11). In detail, 16 µl citrated whole blood was incubated with the following antibody (ab) cocktail for 30 min at 37 °C: 2.5 µl FITC-labeled anti-CD42b (emfret), 1.5 µl PerCP-labeled anti-CD45 (Biolegend), 2.0 µl BV421-labelled anti-CD11b (Biolegend), 1.5 µl Alexa fluor-labeled anti-CD62P (BD), 1.5 µl PE-labeled JON-A (emfret), and 2.0 µl PE-Cy7-labeled anti-Ly6G/6C (Biolegend). Next, 3 µl of the stained samples were diluted in 500 µl 1 x CellFix (BD). Flow cytometry was performed within 4 h after sample fixation.

Tissue staining techniques for histological analysis

Immunohistochemistry staining and scoring techniques (11-13) were used to investigate tissue samples of murine peritoneum, kidney, and liver for PNA sequestration, erythrocyte extra-vasation, and tissue damage.

Immunohistochemistry of platelets and neutrophils

Tissue sections of the peritoneum, kidney, and liver were evaluated for PNA sequestration by immunohistochemistry staining according to the principles of a previously described method (11). Tissue sections of 3 µm were fixed and blocked with methanol and hydrogen peroxidase (Sigma). Antigens were retrieved with unmasking buffer (Vector laboratories, California, USA). Slides were then blocked with Avidin (Vector Laboratories, California, USA) and incubated with neutrophil rabbit–anti-mouse Ly6b primary antibody (Serotec, North Carolina, USA) and platelet rat–anti-mouse CD41 (Santa Cruz, California, USA), followed by an overnight incubation step in biotin-blocking buffer (Vector Laboratories) at 4 °C. After washing with $PBS^{-/-}$ (Sigma), a rabbit HRP secondary antibody labeled with ABC solution (Vector Laboratories) and a rat biotinilated secondary antibody labeled with DAB Histogreen (BioRad) were applied. All secondary antibody controls were included in the vectastain protocol and used according to the manufacturer's instructions. In slides with embedded tissue, the cell nuclei were stained with fast nuclearRed as counterstain (Vector Laboratories). PNAs were visualized with a 40x fold planar objective mounted on a Leica inverted microscope (Leica, Wetzlar, Germany). Pictures were acquired with a Zeiss Axiocam 305 color camera (Zeiss, Jena, Germany) using Zeiss Axiovision 4.8 software (release 2009).

Erythrocyte staining

Paraffin embedded tissue sections of the peritoneum, kidney, and liver were fixed in acetone, washed and endogenous peroxidase blocked with 3% H_2O_2 before blocking for 30 min with 10% serum at room temperature. After washing, endogenous biotin was blocked (with a Vectastain block kit) and 1:400 primary antibody rat anti-mouse Ter119 (Invitrogen, Darmstadt, Germany) incubated over-night at 4ºC. For developing ABC reagent was incubated at 1:100 dilution for 30 min and DAB incubated until sections turned brown.

Counterstaining of tissue sections was performed with Mayer's Haematoxicilin for 15 s and consequent rinsing in water. For mounting, stained tissue sections were dehydrated in increasing ethanol steps, cleared in xylene and covered with DEPEX.

Erythrocytes were visualized with a 40x fold planar objective mounted on a Leica inverted microscope. Images were acquired with a Axiocam 305 color camera (Zeiss) using Axiovision 4.8 software (Zeiss, release 2009).

Analysis of kidney tissue for inflammation-associated damage

Kidney tissue was analyzed for tissue damage as previously described (12). In short, formalin-fixed and paraffin-embedded tissue sections were stained with hematoxylin-eosin and assessed microscopically. The following semi-quantitative scale was used as previously described (12) to evaluate the degree of tubular necrosis: 0, normal kidney; 1, minimal necrosis (<10% involvement); 2, mild necrosis (10 - <25% involvement); 3, moderate necrosis (25 - 75% involvement); and 4, severe necrosis (>75% involvement).

Analysis of liver tissue for inflammation-associated damage

Liver tissue was analyzed for tissue damage according to a previously described method (13). In short, formalin-fixed and paraffin-embedded tissue sections were stained with hematoxylin-eosin and assessed using a 40x fold planar objective mounted on a Leica inverted microscope. Images were acquired with an Axiocam 305 color camera (Zeiss) using Axiovision 4.8 software (Zeiss, release 2009). Histological changes were scored as previously described (13) based on the parameters "sinusoidal congestion", "cytoplasmic vacuolization", and "parenchymal cell necrosis".

Statistical analysis

Statistical analyses were performed using GraphPad Prism, version 7.03 for Windows 5 (GraphPad Software, San Diego, California, USA) and IBM SPSS® software, version 23.0 (Armonk, NY: IBM Corp). Continuous variables are reported as either mean and standard error of the mean (SEM) or medians and interquartile range depending on the distribution of the data. In addition dot plots are shown for several data sets as indicated.

In detail, the normal distribution of data sets was evaluated by investigating kurtosis, skewness, as well as Q-Q plots and histograms. Data, which were found to be normally distributed are reported as means and SEM. The variables without normal distribution were transformed with a log-transformation to transform skewed data to approximately conform to normality. When a normal distribution was achieved by transformation in logarithms, assessment of statistical differences was performed on the transformed data and the data are shown in graphs as means and SEM. Data for which a normal distribution could not be established by log-transformation are shown in graphs as median and interquartile range

The statistical significance of differences was assessed by one-way variance analysis and post hoc Holm-Sidak's test for continuous normally distributed variables, or by non-parametric Kruskal Wallis test and post hoc Dunn’s test for skewed variables in which normality was not achieved by log-transformation.

Survival data from the CLP experiments are depicted using Kaplan–Meier curves and groups were compared using the log-rank (Mantel–Cox) test. Body temperatures and body weights of the mice who underwent the CLP model were also investigated for treatment-associated effects. Due to the CLP-associated mortality, the data for this analysis contained a considerable quantity of missing values. Therefore, it was decided to analyze weight and temperature changes using a linear mixed regression model and to analyze the repeated

measurement of each mouse. The fixed effects of the model included time and therapy. Random effects of the nested model included each mouse. The variance components were estimated using the Maximum Likelihood Estimation (MLE) method. The unstructured variance-covariance option was used to estimate the variance-covariance components.

A p-value of <0.05 was considered to indicate a statistically significant difference.

References

1. Russwurm S, Vickers J, Meier-Hellmann A, et al. Platelet and leukocyte activation correlate with the severity of septic organ dysfunction. *Shock* 2002;17(4):263-268.

2. Köhler D, Straub A, Weissmuller T, et al. Phosphorylation of vasodilator-stimulated phosphoprotein prevents platelet-neutrophil complex formation and dampens myocardial ischemia-reperfusion injury. *Circulation* 2011;123(22):2579-2590.

3. Deitch EA. Rodent models of intra-abdominal infection. *Shock* 2005;24 Suppl 1:19-23.

4. Hohmann JD, Wang X, Krajewski S, et al. Delayed targeting of CD39 to activated platelet GPIIb/IIIa via a single-chain antibody: breaking the link between antithrombotic potency and bleeding? *Blood* 2013;121(16):3067-3075.

5. Ziegler M, Hohmann JD, Searle AK, et al. A single-chain antibody-CD39 fusion protein targeting activated platelets protects from cardiac ischaemia/reperfusion injury. *Eur Heart J* 2018;39(2):111-116.

6. Goldenberg NM, Steinberg BE, Slutsky AS, et al. Broken barriers: a new take on sepsis pathogenesis. *Science translational medicine* 2011;3(88):88ps25.

7. Iba T, Levy JH. Inflammation and thrombosis: roles of neutrophils, platelets and endothelial cells and their interactions in thrombus formation during sepsis. *J Thromb Haemost* 2018;16(2):231-241.

8. Schlegel M, Granja T, Kaiser S, et al. Inhibition of neogenin dampens hepatic ischemia-reperfusion injury. *Crit Care Med* 2014;42(9):e610-619.

9. Csoka B, Nemeth ZH, Rosenberger P, et al. A2B adenosine receptors protect against sepsis-induced mortality by dampening excessive inflammation. *J Immunol* 2010;185(1):542-550.

10. Rittirsch D, Huber-Lang MS, Flierl MA, et al. Immunodesign of experimental sepsis by cecal ligation and puncture. *Nature protocols* 2009;4(1):31-36.

11. Granja TF, Köhler D, Schad J, et al. Adenosine Receptor Adora2b Plays a Mechanistic Role in the Protective Effect of the Volatile Anesthetic Sevoflurane during Liver Ischemia/Reperfusion. *Anesthesiology* 2016;125(3):547-560.

12. Sashindranath M, Dwyer KM, Dezfouli S, et al. Development of a novel strategy to target CD39 antithrombotic activity to the endothelial-platelet microenvironment in kidney ischemia-reperfusion injury. *Purinergic Signal* 2017;13(2):259-265.

13. Suzuki S, Toledo-Pereyra LH, Rodriguez FJ, et al. Neutrophil infiltration as an important factor in liver ischemia and reperfusion injury. Modulating effects of FK506 and cyclosporine. *Transplantation* 1993;55(6):1265-1272.

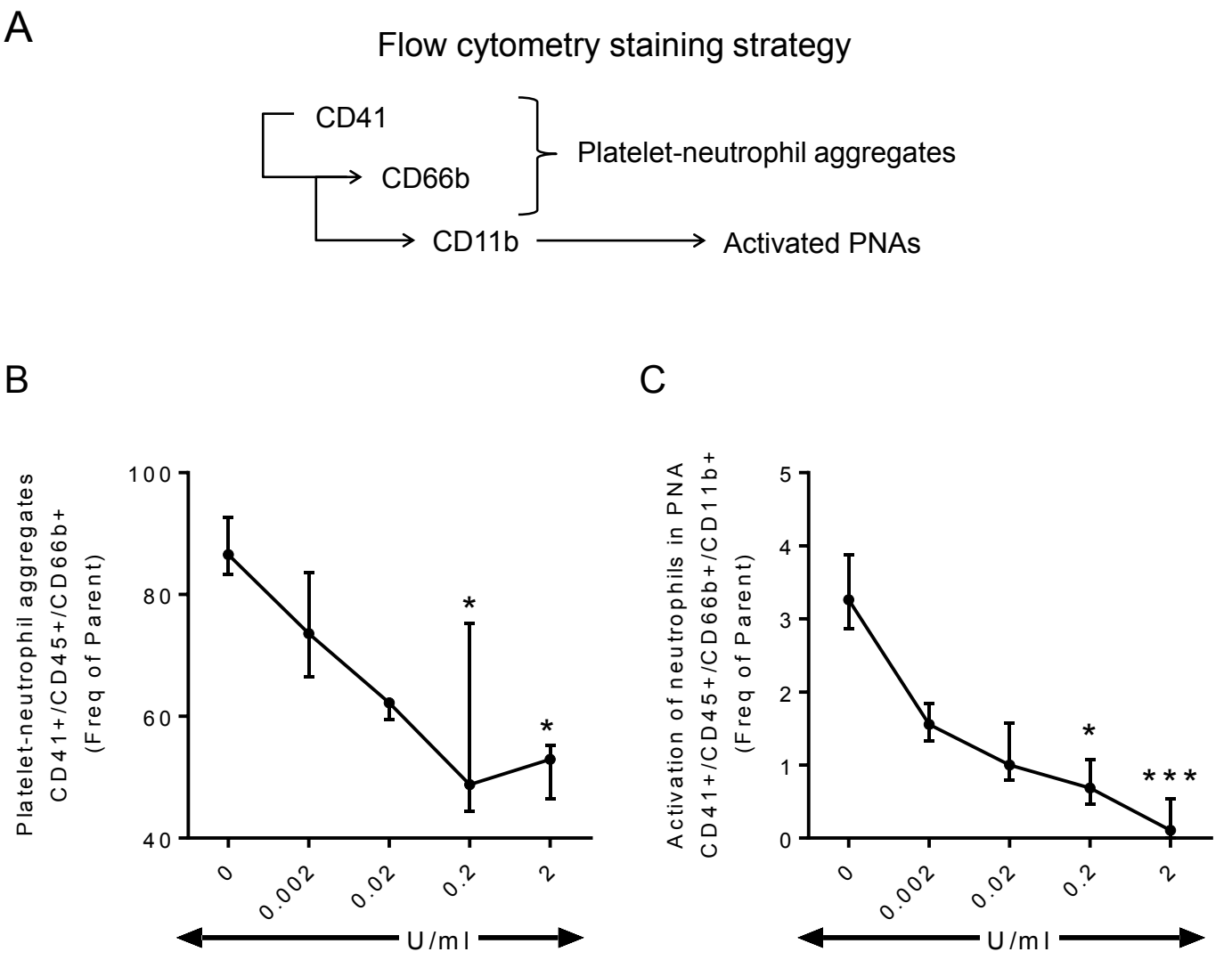

Figure S1: Potato apyrase dose-dependently decreases platelet-neutrophil aggregate formation and neutrophil activation. Citrated whole blood was incubated with ADP (20 µM) and different concentrations of potato apyrase (PA). The formation of platelet–neutrophil aggregates (PNA) and activation of PNA-bound neutrophils were analyzed via flow cytometry. A: Flow cytometry staining strategy. Platelets and leukocytes were detected according to typical scatter profiles and positive staining for the antibodies anti-CD41-FITC, anti-CD45-PerCp, and anti-CD66b-PE/Cy7. Activation of PNA-bound neutrophils was analyzed using an anti-CD11b-BV antibody. Dose-dependent inhibition of PNA formation (B) and expression of the activation marker CD11b on neutrophils was observed (C). A PA concentration of 2 U/ml promotes almost complete inhibition of CD11b expression on neutrophils (C). Data are shown as medians and interquartile range; n=4/group; p-values are derived from the Kruskal Wallis test and Dunn's post hoc test; * = $p<0.05$ *** = $p<0.001$ vs. group "0 U/ml" as control.

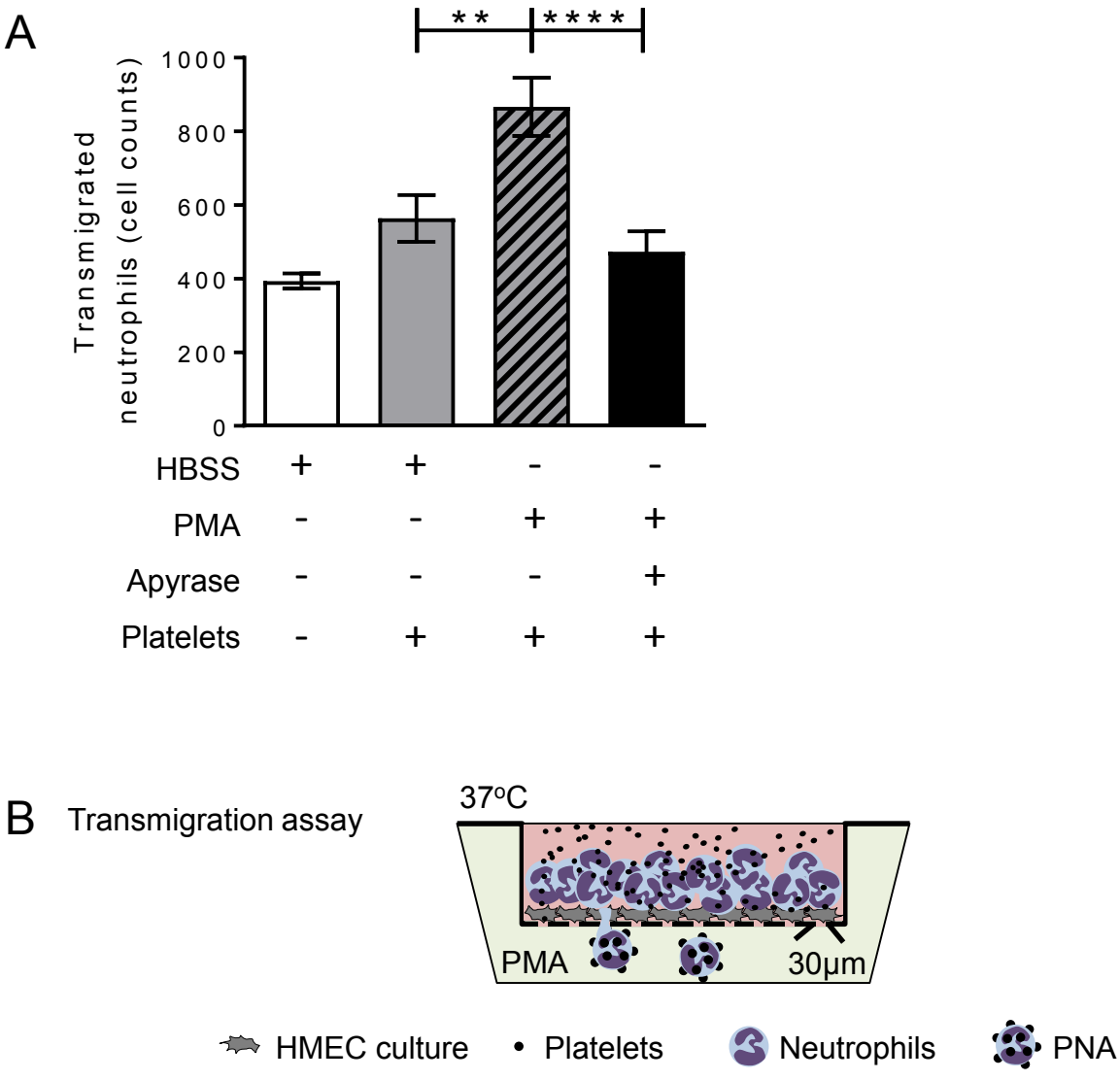

Figure S2: Potato apyrase decreases transendothelial neutrophil transmigration under inflammatory conditions in vitro.

A and B: Transmigration of human neutrophils across HMEC-1 cells in the presence and absence of platelets was analyzed using a transendothelial migration assay. Platelets, potato apyrase and phorbol-12-myristat-e13-acetate (PMA) were added as indicated. Data are shown as means ± standard error of the mean of n=6 experiments/group; the p-value is derived from one-way analysis of variance (ANOVA) and Holm-Sidak's multiple comparison test; ** = $p<0.01$; **** = $p<0.0001$

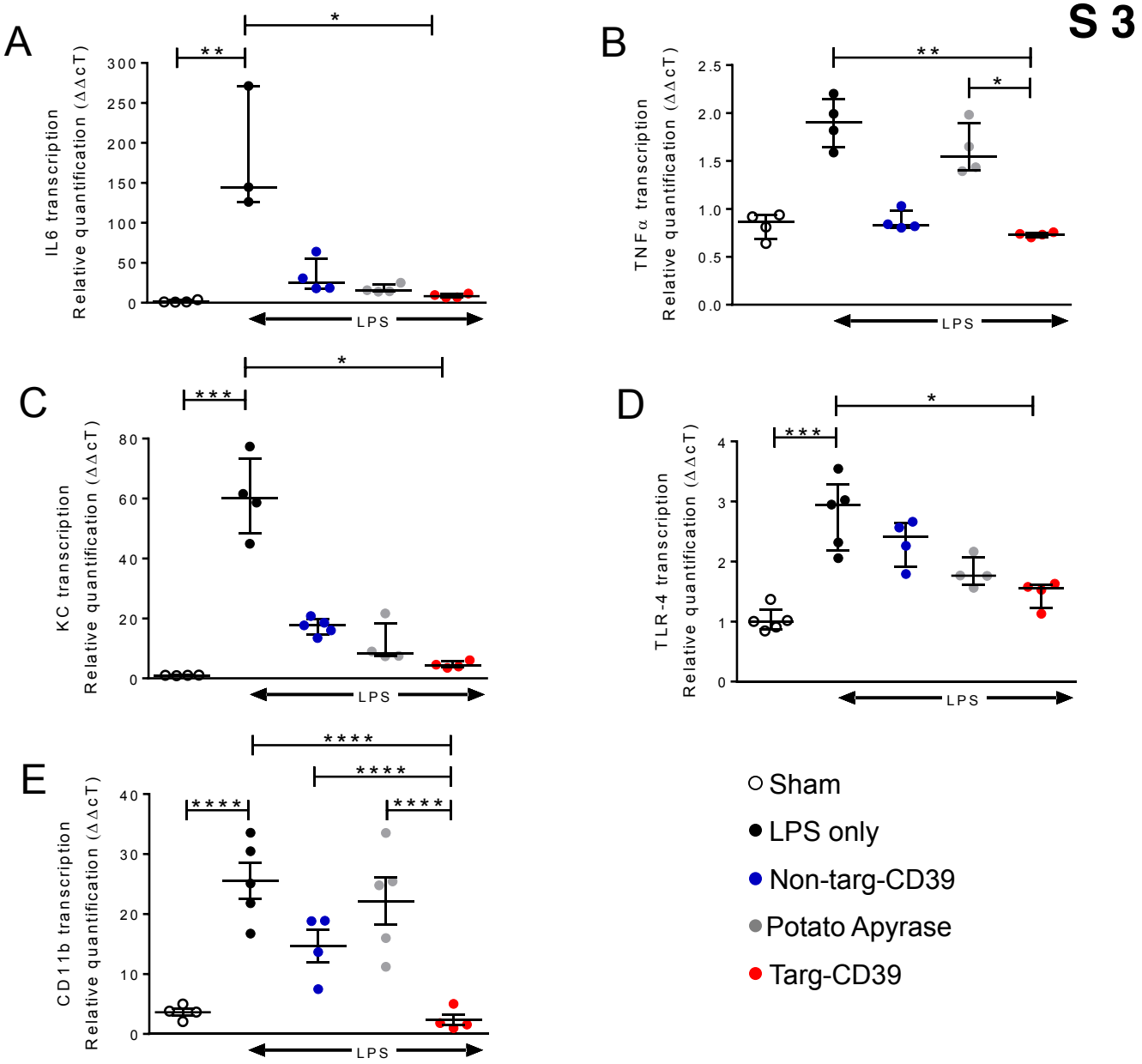

Figure S3: Effects of targ-CD39, non-targ-CD39, and potato apyrase on transcription of IL-6, TNF-α, KC, TLR-4 and CD11b in the peritoneum during LPS-induced peritonitis in mice.

The platelet-targeted molecule targ-CD39 (0.4 µg/g BW), its control substance non-targ-CD39 (in equimolar concentration of 0.4 µg/g BW), or potato apyrase (PA) (0,04 U/g BW) were administered intravenously as indicated to C57BL/6NCrl mice. Lipopolysaccharide (LPS) was administered intraperitoneally to induce peritonitis and systemic inflammation. Four hours after administration of experimental agents, peritoneum samples were harvested from mice for further analysis. The transcription of the proinflammatory cytokines interleukin 6 (IL-6), TNF-α, and keratinocyte chemoattractant (KC) as well as transcription of TLR-4 and CD11b in peritoneal tissue was analyzed using PCR. A: Targ-CD39 decreased IL-6 transcription. Non-targ-CD39 and PA had no significant effect on IL-6 transcription. B: Targ-CD39 decreased TNF-α transcription versus control and PA-treated samples. PA and non-targ-CD39 had no significant effect on TNF-α transcription. C: Targ-CD39 decreased KC transcription. Non-targ-CD39 and PA had no significant effect on KC transcription. D: Targ-CD39 decreased TLR-4 transcription. Non-targ-CD39 had no significant effect on TLR-4 transcription. Data in A-D are shown as medians, interquartile ranges and dot plots from n=4-5 experiments per group. Assessment of statistical differences was performed using the Kruskal Wallis test and Dunn's post hoc test. E: Targ-CD39 decreased CD11b transcription versus control and versus non-targ-CD39- and PA-treated samples. PA and non-targ-CD39 had no significant effect on CD11b transcription. For analysis of differences between data sets variables were transformed with a log-transformation to approximately conform data to normality. Statistical significance of differences between the log-transformed data sets was assessed by one-way analysis of variance and the Holm-Sidak post hoc test. Data are shown as means with standard error of the mean and dot plots from n=4-5 experiments per group; * = $p<0.05$; ** = $p<0.01$; *** = $p<0.001$; **** = $p<0.0001$.

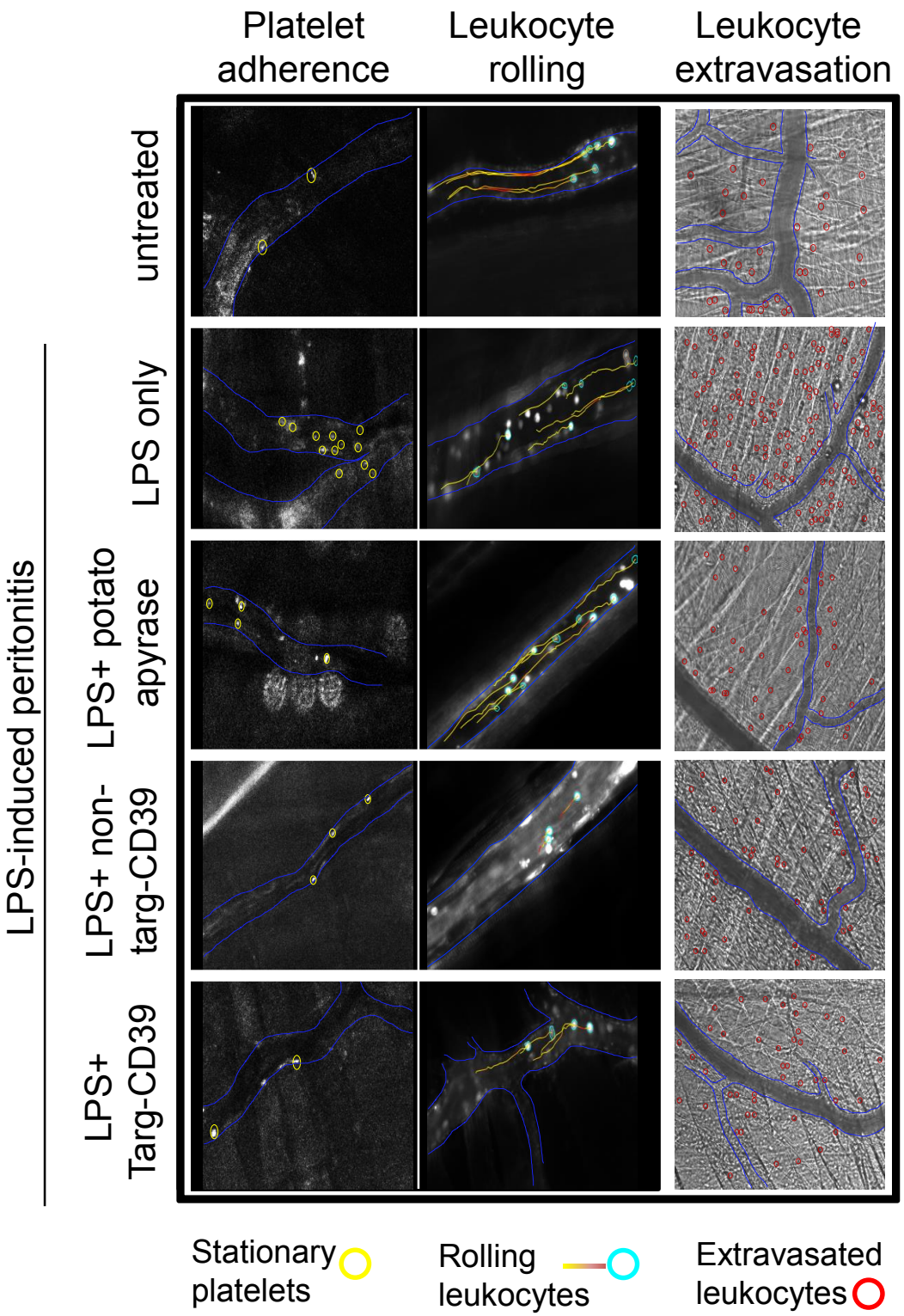

Figure S4: Representative intravital microscopy images depicting platelet-endothelium adherence, leukocyte rolling, and leukocyte extravasation in the cremaster musculature of C57BL/6NCrl mice. Systemic inflammation was induced by intraperitoneal administration of LPS. The platelet-targeted molecule targ-CD39 (0.4 µg/g BW), its control substance non-targ-CD39 (in equimolar concentration of 0.4 µg/g BW), or potato apyrase (0,04 U/g BW) were administered as indicated. Platelets were stained with a platelet-specific FITC-labeled X488 antibody and leukocytes were stained with rhodamine. Imaging was performed four hours after administration of LPS and experimental agents. Platelets and leukocytes were visualized using intravital fluorescence microscopy. Extravasated leukocytes were visualized in brightfield microscopy. Endothelium-adherent platelets are marked with yellow circles. Rolling leukocytes and their tracks are indicated in turquoise. The length of the leukocyte tracks (marked in yellow) indicates the distance, which the respective leukocyte travelled during an observation period of 30 seconds. Extravasated leukocytes are marked with red circles.

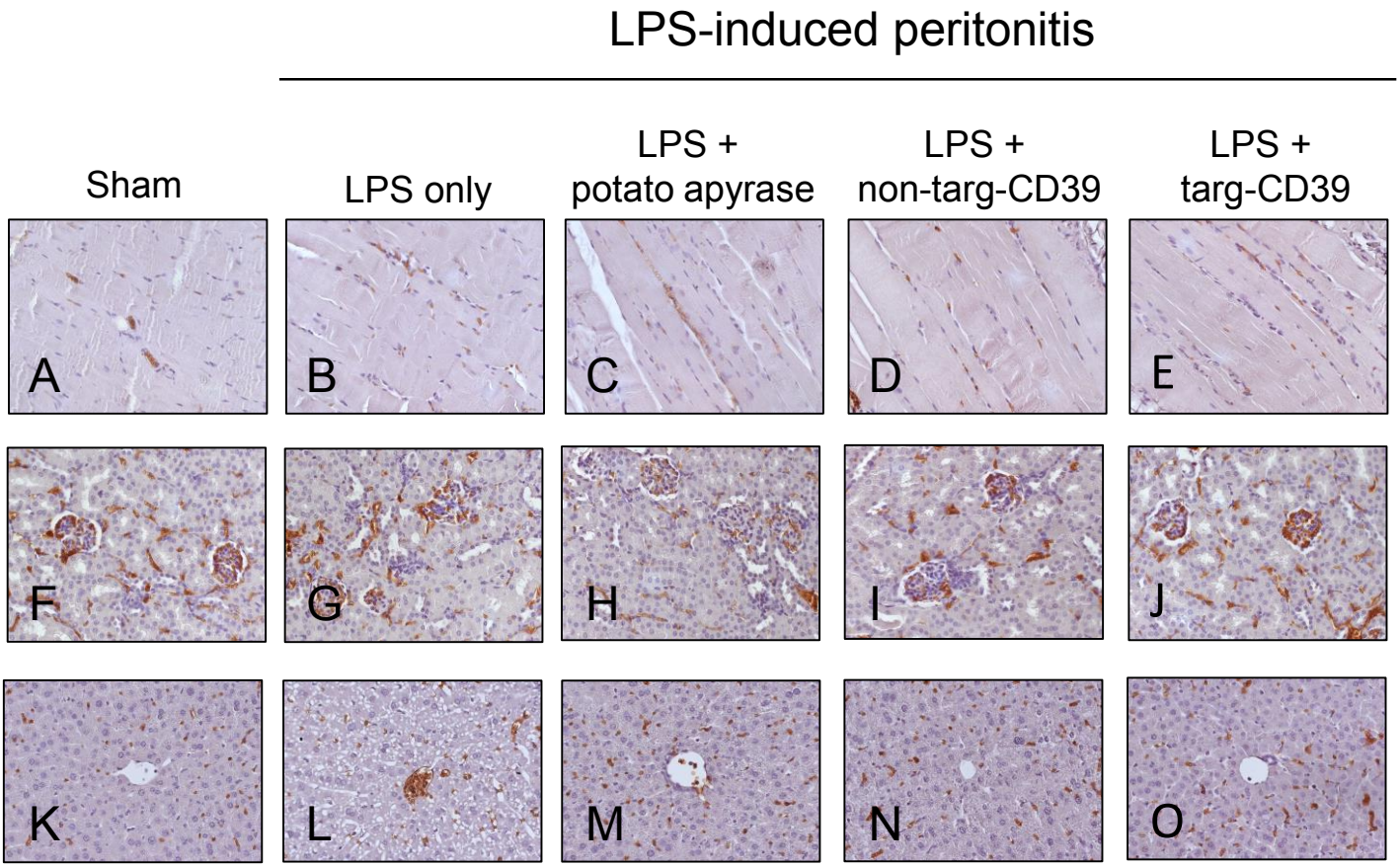

Figure S5: Targ-CD39, non-targ-CD39, and potato apyrase do not induce bleeding inside peritoneum, kidney, and liver during LPS-induced peritonitis in mice

The platelet-targeted molecule targ-CD39 (0.4 µg/g BW), its control substance non-targ-CD39 (in equimolar concentration of 0.4 µg/g BW), or potato apyrase (0,04 U/g BW) were administered as indicated intravenously to C57BL/6NCrl mice. Lipopolysaccharide (LPS) was administered intraperitoneally to induce peritonitis and systemic inflammation. Four hours after administration of experimental agents, tissue samples of peritoneum, liver, and kidney were harvested from mice (n=5/treatment group) for further analysis. Erythrocytes were stained using an anti-mouse Ter119 antibody and were visualized using immunohistochemistry and microscopy techniques. Erythrocytes appear in brown color in the respective images. A-E: Representative microscopy images of the peritoneum depicting the distribution of erythrocytes in the specific treatment groups. F-J: Representative microscopy images of the kidney depicting the distribution of erythrocytes in the specific treatment groups. K-O: Representative microscopy images of the liver depicting the distribution of erythrocytes in the specific treatment groups. No relevant erythrocyte extravasation as a sign for bleeding and no relevant differences between treatment groups were observed in any of the investigated tissues.

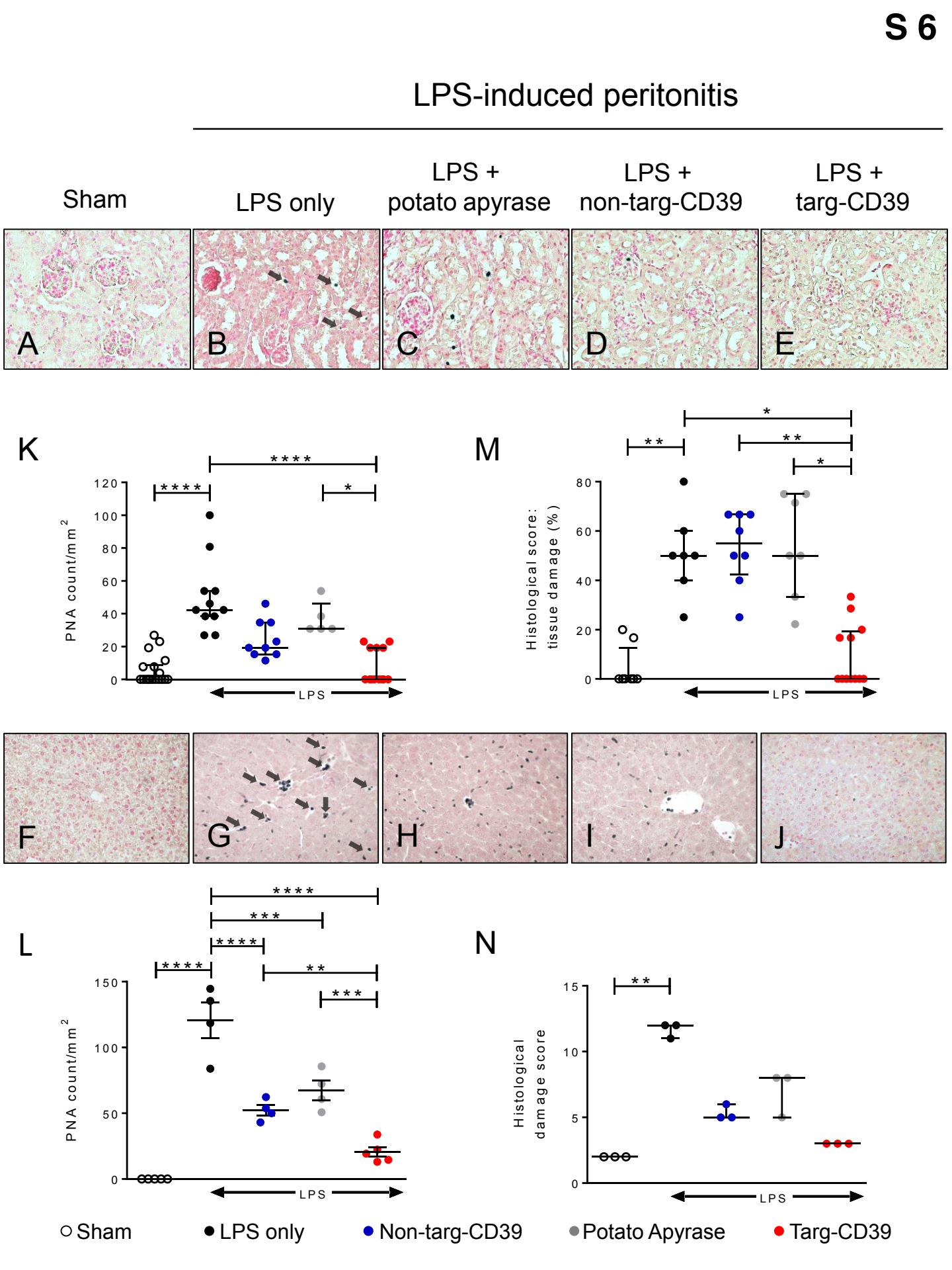
LPS-induced peritonitis
Sham
LPS only
LPS + potato apyrase
LPS + non-targ-CD39
LPS + targ-CD39
A
B
C
D
E
K
PNA count/mm2
LPS
M
Histological score: tissue damage (%)
LPS
F
G
H
I
J
L
PNA count/mm2
LPS
N
Histological damage score
LPS
Sham
LPS only
Non-targ-CD39
Potato Apyrase
Targ-CD39

Figure S6: Targ-CD39 decreases microvascular platelet-neutrophil aggregate sequestration and tissue damage in the kidney and liver during LPS-induced peritonitis.
The platelet-targeted molecule targ-CD39 (0.4 µg/g BW), its control substance non-targ-CD39 (in equimolar concentration of 0.4 µg/g BW), or potato apyrase (PA) (0,04 U/g BW) were administered as indicated intravenously to C57BL/6NCrl mice. Lipopolysaccharide (LPS) was administered intraperitoneally to induce peritonitis and systemic inflammation. Four hours after administration of experimental agents, kidney and liver tissue samples were harvested from mice for further analysis. A-E: Sequestered platelet–neutrophil aggregates (PNA) were visualized in the kidney using immunohistochemistry and microscopy techniques (representative tissue stainings shown at 40-fold magnification). PNA are exemplarily marked by black arrows in B. F-J: Sequestered platelet–neutrophil aggregates (PNA) were visualized in the liver using immunohistochemistry and microscopy techniques (representative tissue stainings shown at 40-fold magnification). PNA are exemplarily marked by black arrows in G. K: In the kidney targ-CD39 decreased PNA sequestration significantly compared to control and PA-treated samples. Non-targ-CD39 and PA had no significant inhibitory effect on PNA sequestration. Data are shown as medians, interquartile ranges, and dot plots. Assessment of statistical differences was performed using the Kruskal Wallis test and Dunn's post hoc test. L: In the liver the inhibitory effect of targ-CD39 on PNA sequestration was stronger then the effect of non-targ-CD39 and PA.
Tissue damage was assessed using microscopy according to histological scoring systems. Data are shown as mean with standard error of the mean and dot plots. Statistical significance of differences between data sets was assessed by one-way analysis of variance and Holm-Sidak's post hoc test. M: In the kidney targ-CD39 significantly decreased organ damage compared to non-targ-CD39, PA, and control samples. Non-targ-CD39 and PA had no protective effect. Data are shown as medians and interquartile range and dot plots. Assessment of statistical differences was performed using the Kruskal Wallis test and Dunn's post hoc test. N: In the liver neither treatment (targ-CD39, non-targ-CD39, PA) had a significant inhibitory effect on organ damage. Data are shown as medians and interquartile range and dot plots. Assessment of statistical differences was performed using the Kruskal Wallis test and Dunn's post hoc test. Data in K - N are derived from n=3 experiments/group; * = $p<0.05$; ** = $p<0.01$; *** = $p<0.001$; **** = $p<0.0001$.

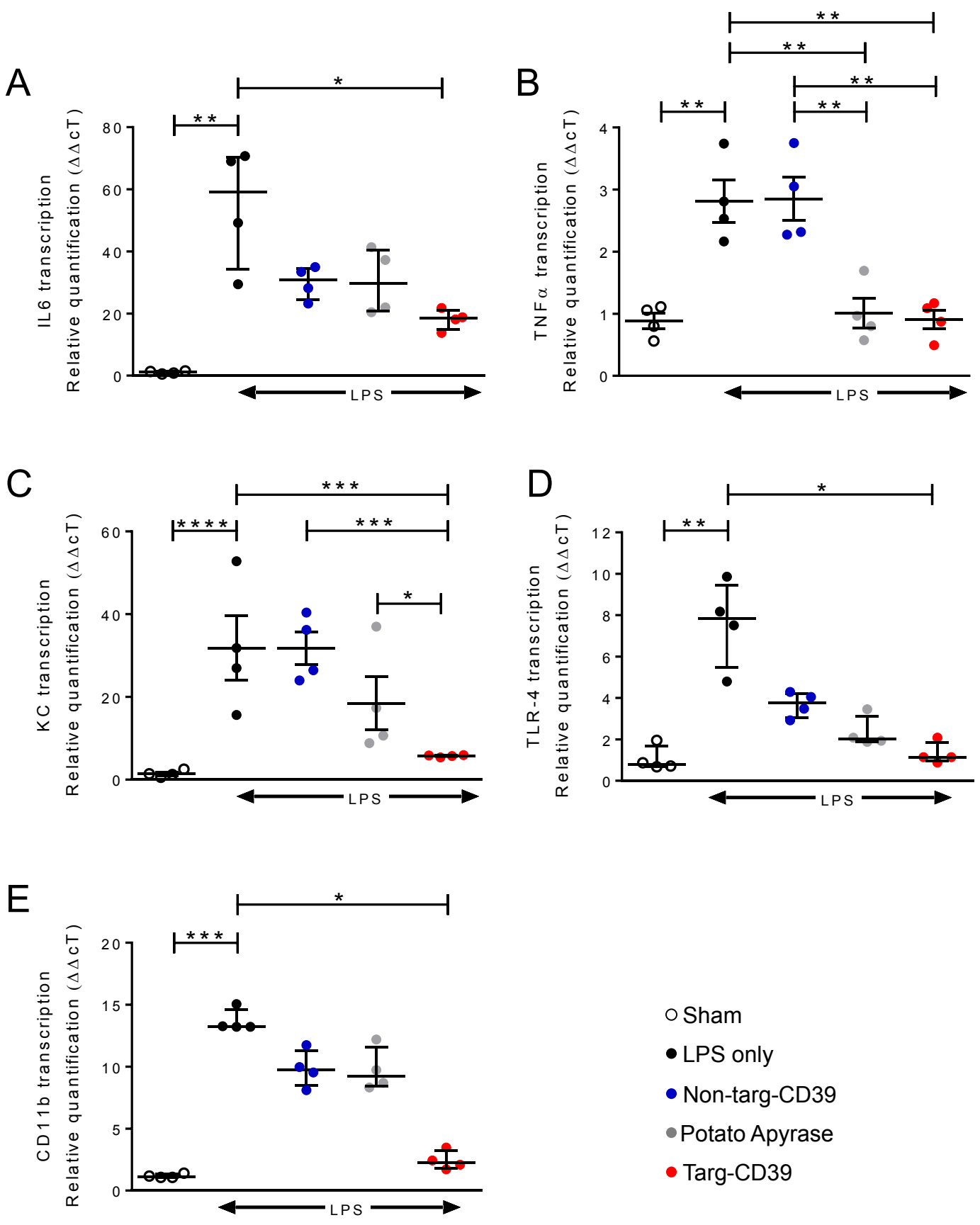
A
IL6 transcription
Relative quantification (ΔΔcT)
LPS
B
TNFα transcription
Relative quantification (ΔΔcT)
LPS
C
KC transcription
Relative quantification (ΔΔcT)
LPS
D
TLR-4 transcription
Relative quantification (ΔΔcT)
LPS
E
CD11b transcription
Relative quantification (ΔΔcT)
LPS
Sham
LPS only
Non-targ-CD39
Potato Apyrase
Targ-CD39

Figure S7: Effects of targ-CD39, non-targ-CD39, and potato apyrase on transcription of IL-6, TNF-α, KC, TLR-4 and CD11b in the kidney during LPS-induced peritonitis in mice. The platelet-targeted molecule targ-CD39 (0.4 µg/g BW), its control substance non-targ-CD39 (in equimolar concentration of 0.4 µg/g BW), or potato apyrase (PA) (0,04 U/g BW) were administered intravenously as indicated to C57BL/6NCrl mice. Lipopolysaccharide (LPS) was administered intraperitoneally to induce peritonitis and systemic inflammation. Four hours after administration of experimental agents, kidney samples were harvested from mice for further analysis. The transcription of the proinflammatory cytokines interleukin 6 (IL-6), TNF-α, and keratinocyte chemoattractant (KC) as well as transcription of TLR-4 and CD11b in kidney tissue was analyzed using PCR. A: Targ-CD39 decreased IL-6 transcription. Non-targ-CD39, and PA had no significant inhibitory effect on IL-6 transcription. Data are shown as medians, interquartile ranges, and dot plots. Assessment of statistical differences was performed using the Kruskal Wallis test and Dunn's post hoc test. B: Targ-CD39 and PA decreased TNF-α transcription. Non-targ-CD39 had no significant effect on TNF-α transcription. Data are shown as dot plots and means with standard error of the mean (SEM). For analysis of differences between data sets variables were transformed with a log-transformation to approximately conform data to normality. Statistical significance of differences between the log-transformed data sets was assessed by one-way analysis of variance and the Holm-Sidak post hoc test. C: Targ-CD39 decreased KC transcription. Non-targ-CD39 and PA had no significant effect on KC transcription. Data are shown as dot plots and means with SEM. For analysis of differences between data sets variables were transformed with a log-transformation to approximately conform data to normality. Statistical significance of differences between the log-transformed data sets was assessed by one-way analysis of variance and the Holm-Sidak post hoc test. D: Targ-CD39 decreased TLR-4 transcription. Non-targ-CD39 and PA had no significant effect on TNF-α transcription. Data are shown as medians, interquartile ranges, and dot plots. Assessment of statistical differences was performed using the Kruskal Wallis test and Dunn's post hoc test. E: Targ-CD39 decreased CD11b transcription. Non-targ-CD39 and PA had no significant effect on CD11b transcription. Data are shown as medians with interquartile range and dot plots. Assessment of statistical differences was performed using the Kruskal Wallis test and Dunn's post hoc test. Data are derived from n=4 experiments per group; * = $p<0.05$; ** = $p<0.01$; *** = $p<0.001$.

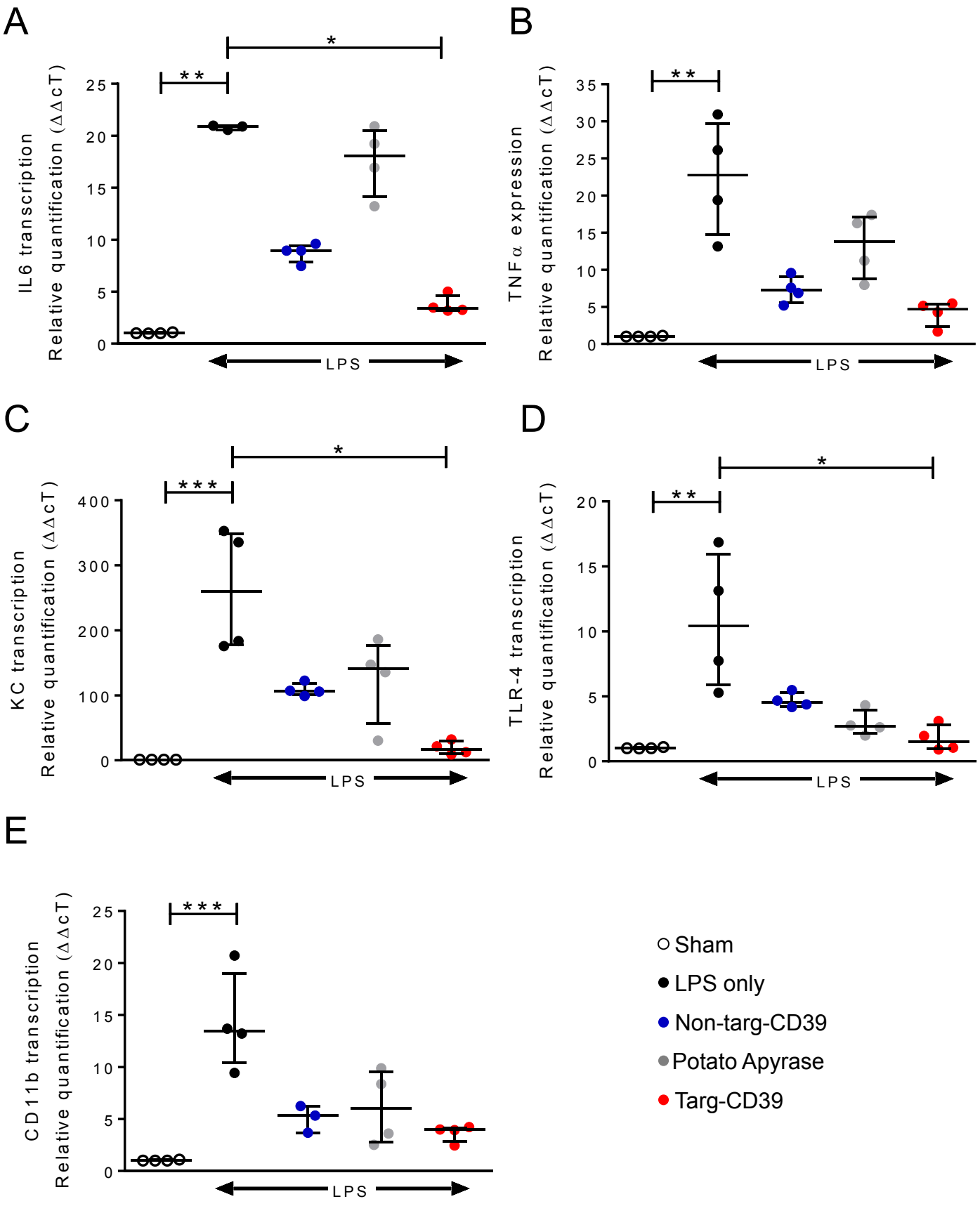
A
IL6 transcription
Relative quantification (ΔΔcT)
25
20
15
10
5
0
**
*
LPS
B
TNFα expression
Relative quantification (ΔΔcT)
35
30
25
20
15
10
5
0
**
LPS
C
KC transcription
Relative quantification (ΔΔcT)
400
300
200
100
0
***
*
LPS
D
TLR-4 transcription
Relative quantification (ΔΔcT)
20
15
10
5
0
**
*
LPS
E
CD11b transcription
Relative quantification (ΔΔcT)
25
20
15
10
5
0
***
LPS
Sham
LPS only
Non-targ-CD39
Potato Apyrase
Targ-CD39

Figure S8: Effects of targ-CD39, non-targ-CD39, and potato apyrase on transcription of IL-6, TNF-α, KC, TLR-4 and CD11b in the liver during LPS-induced peritonitis in mice.

The platelet-targeted molecule targ-CD39 (0.4 µg/g BW), its control substance non-targ-CD39 (in equimolar concentration of 0.4 µg/g BW), or potato apyrase (PA) (0,04 U/g BW) were administered intravenously as indicated to C57BL/6NCrl mice. Lipopolysaccharide (LPS) was administered intraperitoneally to induce peritonitis and systemic inflammation. Four hours after administration of experimental agents, liver samples were harvested from mice for further analysis. The transcription of the proinflammatory cytokines interleukin 6 (IL-6), TNF-α, and keratinocyte chemoattractant (KC) as well as transcription of TLR-4 and CD11b in liver tissue was analyzed using PCR. A: Targ-CD39 decreased IL-6 transcription. PA and non-targ-CD39 had no significant effect on on IL-6 transcription. B: Neither treatment (targ-CD39, non-targ-CD39, PA) had a significant effect on TNF-α transcription. C: Targ-CD39 decreased KC transcription. PA and non-targ-CD39 had no significant effect on KC transcription. D: Targ-CD39 decreased TLR-4 transcription. PA and non-targ-CD39 had no significant effect on TLR-4 transcription E: Neither treatment (targ-CD39, non-targ-CD39, PA) had a significant effect on CD11b transcription. Data are shown as medians with interquartile range and dot plots from n=4 experiments per group. Assessment of statistical differences was performed using the Kruskal Wallis test and Dunn's post hoc test.; * = $p<0.05$; ** = $p<0.01$; *** = $p<0.001$.

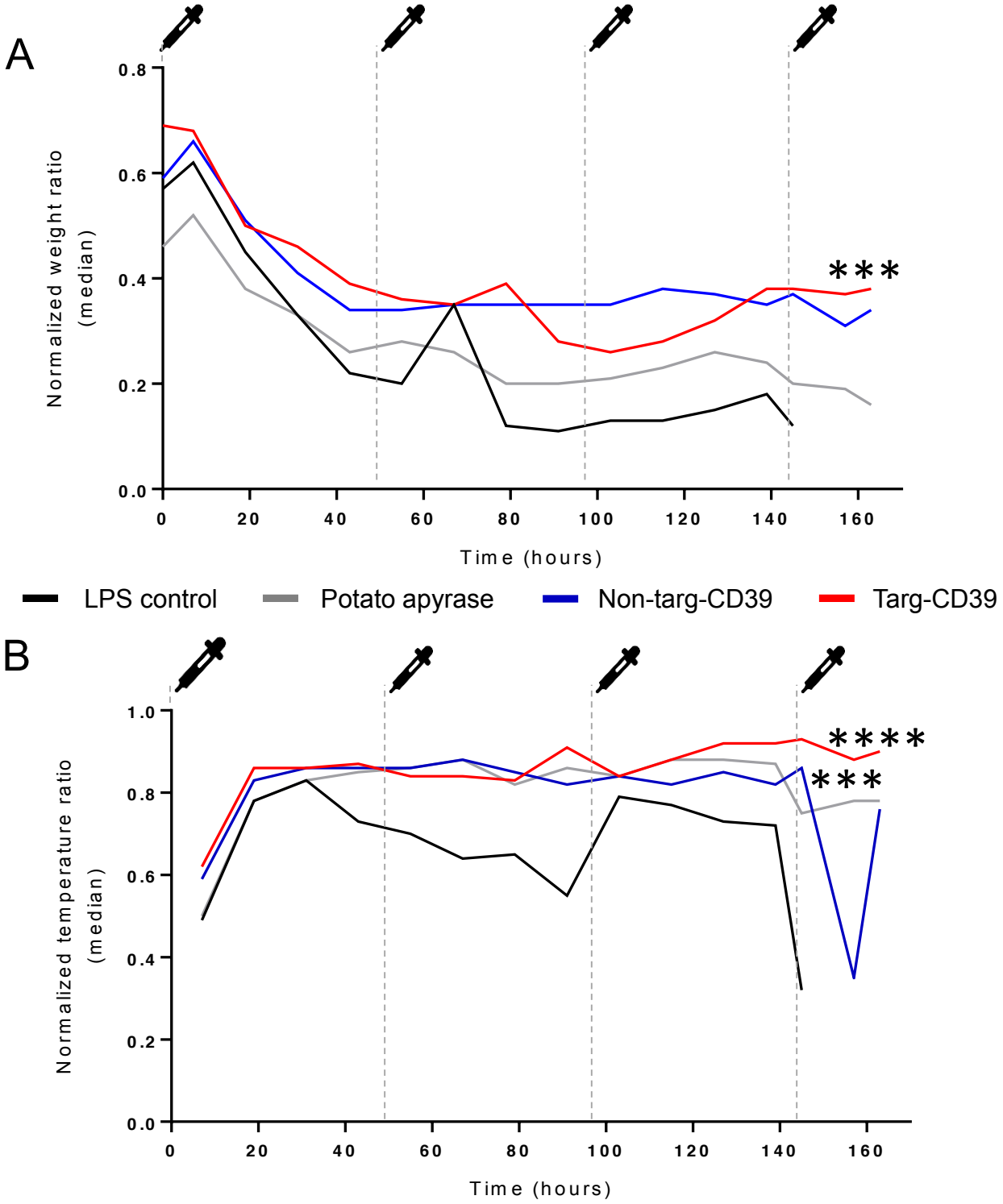

Figure S9: Effects of targ-CD39, non-targ-CD39, and potato apyrase on body weights and body temperatures after cecal ligation and puncture in mice.

The cecal ligation and puncture procedure was performed with C57BL/6NCrl mice. The platelet-targeted molecule targ-CD39 (0.4 µg/g BW), its control substance non-targ-CD39 (in equimolar concentration of 0.4 µg/g BW), or potato apyrase (0,04 U/g BW)) were administered intravenously at the indicated time points ("needle symbol"). Weight and temperature changes were analyzed using a linear mixed regression model.

A: Body weights of mice were significantly higher with targ-CD39 treatment (*** = p=0.004 versus control) but not with potato apyrase treatment (p=0.051 versus control) and non-targ-CD39 treatment (p=0.081 versus control).

B: Body temperatures of mice were significantly higher with targ-CD39 treatment (**** = p<0.0001 versus control) and with non-targ-CD39 (*** = p=0.001 versus control) but not with potato apyrase (p=0.129 versus control).

Data are derived from experiments of 12-15 mice/group; the depicted curves are derived from normalized median values of the respective treatment group.

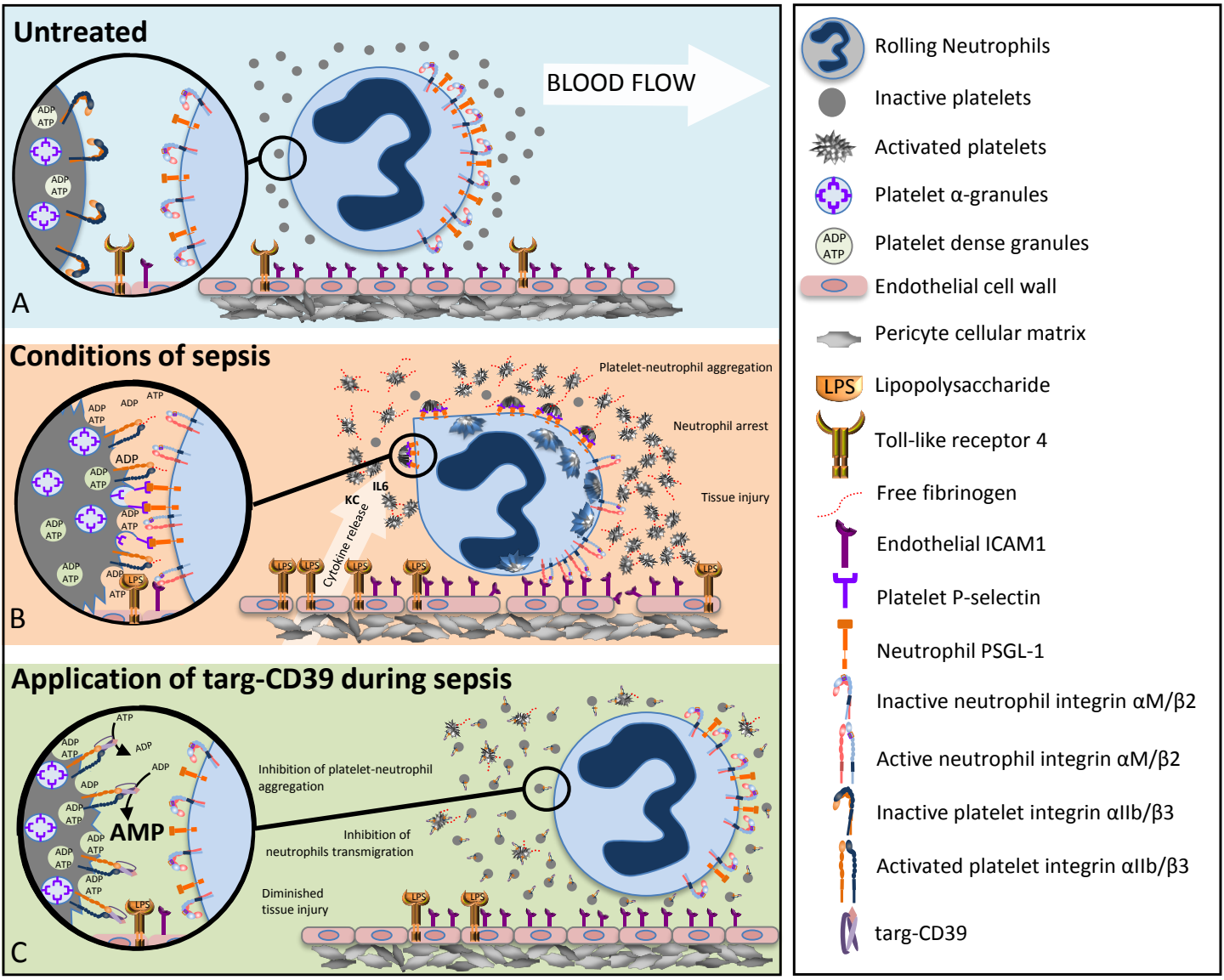

Figure S10: Effect of targ-CD39 on platelet–neutrophil interaction under conditions of sepsis. A: Under physiological conditions without influence of proinflammatory or pro-thrombotic stimuli, platelet αIIb/β3 (GPIIb/IIIa) and neutrophil αM/β2 integrins are in a low-affinity binding state for their ligands. P-selectin is kept in platelet alpha granules and adenosinetriphosphate (ATP), as well as adenosinediphosphate (ADP), in platelet-dense granules. Overall, platelets and neutrophils do not bind to each other and do not adhere to endothelial cells. B: Under conditions of sepsis (here depicted by the presence of lipopolysaccharide (LPS)) toll-like receptor 4 (TLR4) expression and LPS–TLR4 binding increases. Furthermore, local and systemic release of pro-inflammatory cytokines increases. Platelets become activated and release their ATP and ADP stores, while the conformation of the αIIb/β3 integrin changes from a low-affinity to a high-affinity binding state for fibrinogen, which mediates the formation of platelet-platelet aggregates. In addition, platelet P-selectin is expressed on the outer platelet cell membrane. P-selectin binds to neutrophil P-selectin glycoprotein ligand 1 (PSGL-1) and thereby promotes platelet–neutrophil aggregate (PNA) formation. PNA precipitate inside the vascular bedding, with activated αM/β2 binding to endothelial intercellular adhesion molecule 1 (ICAM-1). This promotes transmigration of neutrophils through the endothelial barrier into surrounding tissue. C: Targ-CD39 consists of CD39 recombinantly fused to a single-chain antibody (scFv) which is specific for the activated conformation of the platelet integrin GPIIb/IIIa. Under conditions of LPS-induced peritonitis, targ-CD39 accumulates at activated platelets and splits ATP and ADP into AMP, thereby promoting adenosine generation. Targ-CD39 reduces pro-inflammatory activation of platelets and neutrophils, platelet–neutrophil–endothelium binding, and neutrophil translocation.